Particle Production and Flow at SIS Energies

N. Herrmann [a] [b], FOPI Collaboration

[a]Gesellschaft für Schwerionenforschung, Darmstadt, Germany

[b]Physikalisches Institut der Universität Heidelberg, Heidelberg, Germany

An overview is given over recent measurement of flow and particle production in the energy range from 0.1 to 2 AGeV. Excitation functions for the directed sideward and the azimuthally symmetric transverse flow are presented and show the importance of flow phenomena in this incident energy regime. Rapidity density distributions are indicative of a system size dependence of the stopping process. The role of strange particles as a probe for the hot and dense phase of hadronic matter is discussed with respect to the production and propagation. The spectra of Kaons indicate an equilibration with the surrounding baryons during the expansion while their directed flow pattern is different from that of the nucleons.

1. Introduction

Nuclear matter at densities of a few times the ground state density ($\rho \leq 3\rho_\circ$) and at temperatures well below the Hagedorn temperature ($T \leq 100MeV$) is a system of strongly interacting hadrons whose bulk properties are still poorly understood. The study of hadronic matter offers the possibility to test fundamental properties of QCD. Recent theoretical work suggests that effects of chiral symmetry restoration could give rise to dropping masses in the nuclear medium and should already be visible at relatively low densities [1–5]. In addition the hadronic matter state is the final state of any possibly produced quark-gluon-plasma state and should be reasonably well known in order to be able to detect a transition into a different phase. The properties of hadronic matter are, however, not easily accessible. Hadronic matter can only be produced in relativistic heavy ion collisions and the theoretical analysis based on transport equations is complex and has to take into account the dynamical evolution as well as the elementary processes. The outcome of the reaction is not only determined by the mean field, the so called nuclear matter equation-of-state, but at the same time by the properties of the constituents that might be excited and form resonance matter. The multitude of dependences makes it essentially impossible to relate specific properties to a single experimentally measurable observable. The predictive power of the theory needs to be tested by comparing simultaneously to several independent experimental observables. Among them strangeness production and propagation is now experimentally accessible and found great theoretical interest [6–10].

With the installation of second generation experiments (EOS [11], FOPI[12], KaoS[13], TAPS[14]) following the pioneering work at the Bevalac [15–17] much more complete

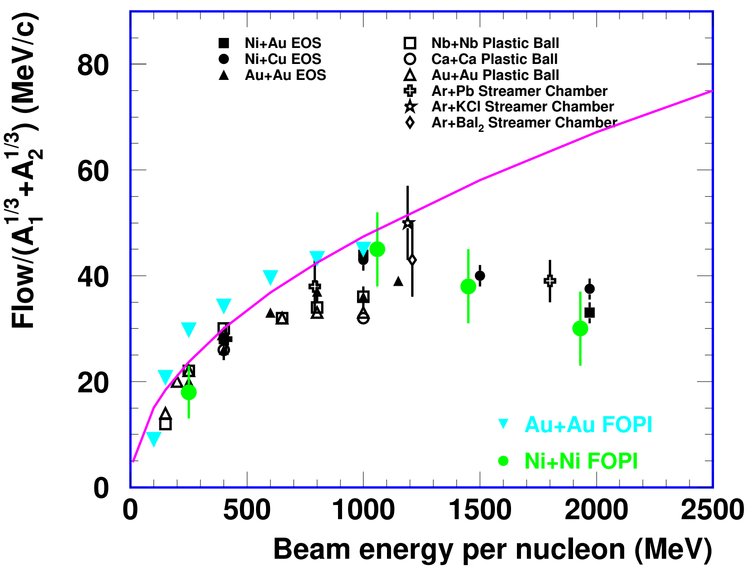

Figure 1. Excitation Function of Sideward Flow

information has become available. This paper tries to summarize the current status of global hadronic observables and hadronic probes, i.e. strange particles, in the energy range from 0.1 to 2 AGeV and is organized in the following way: Section 2 describes the excitation function of sideward flow. In section 3 the degree of collective motion is estimated from the average kinetic energies and the transverse momentum spectra. Section 4 presents the latest information on stopping. In section 5 the production yields of strange mesons are presented including preliminary new data on the Φ - meson. Section 6 contains the status about the directed sideward flow of strange particles. Finally in section 7 a brief summary is given.

2. Sideward Flow

Sideward flow was proposed long time ago to carry the information about the nuclear matter equation of state [16]. Although it was later found that in addition Fermi momenta of the nucleons and two-body scattering processes drive the sideward flow [18], experimentally it nevertheless remains interesting to measure the excitation function. The current status is depicted in fig.1: Plotted is the slope $F = d < p_x/A > /dy'$ of the average transverse momentum projected into the reaction plane with the normalized laboratory rapidity $y' = y/y_p$ for a variety of symmetric and asymmetric projectile - target combinations. In order to make the different systems comparable to each other a scaling factor of $(A_1^{1/3} + A_2^{1/3})$ as first used by J.Chance et al. [19] and suggested by Lang et al.[20] is applied. The data points originate mostly from the EOS collaboration [19] and are complemented by recent preliminary FOPI data [21]. The events are selected according to the charged particle multiplicity. They were chosen to cover an impact parameter range as defined by the Plastic Ball collaboration with multiplicity bin M3+M4 [22]. The F -values shown in fig.1 represents the flow of the average of H and He fragments only, although

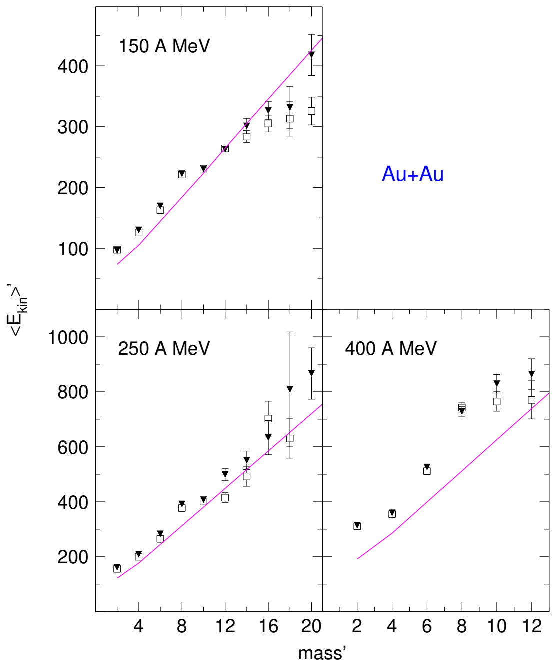

Figure 2. Mean Kinetic Energies of Intermediate Mass Fragments
Mean kinetic energies of fragments with masses determined by $A = 2Z$ in the angular range $25° < \Theta_C M < 45°$ are shown for central collisions [25]. Squares represent the data for an event samples selected by means of the ratio of transverse to longitudinal kinetic energy (ERAT) of 200 mb and azimuthal symmetry, triangles correspond to an ERAT selection of 50 mb. The solid lines are given by blast model fits to the data.

it is known that the heavier fragments shown an even more pronounced flow signature [21,23].

Within the current accuracy of comparison, namely the different acceptances for the global multiplicity and the different particle identification capability of the various experiments, the data are consistent. A clear trend is visible: The sideward flow is rising in the energy range from 150 AMeV to 1 AGeV according to the beam momentum in the CMS. This dependence is depicted by the solid line in Fig. 1. Beyond 1 - 1.2 AGeV the incident energy scaling is broken and the measured values are rather constant or even slightly dropping. The mechanism that is responsible for this behaviour is not yet identified. A systematic comparisons with dynamical models will have to reveal whether the anisotropy of the NN-interaction, the excitation of resonances and / or changes in the stiffness of the equation-of-state are responsibly for the observation. For this task systematic errors can be reduced by applying the proper filter programs of the various experiments.

3. Transverse Flow

The energy contained in the sideward flow is only a small fraction of the available energy and thus does not influence the overall conditions and the thermalisation. The dominating collective flow at incident energies from 0.1 to 1 AGeV is an azimuthally symmetric flow component that can be recognized from its fragment mass dependence for the most central collisions [24]. An example of this effect is presented in fig.2 for the system Au+Au at 150, 250 and 400 AMeV [25]. An almost linear dependence of the average kinetic energies with the ejectile mass is observed. Such a behaviour is indicative for collective flow since under the assumption of a common temperature and a common flow velocity distribution at freeze-out, the average kinetic energy can be written as $<$

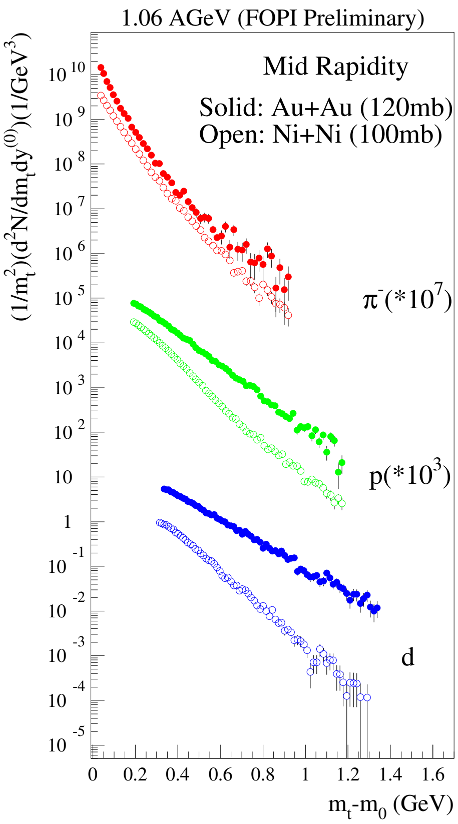

Figure 3. Transverse mass spectra at midrapidity for Pions, Protons and Deuterons in Ni+Ni and Au+Au at 1 AGeV
Pion spectra show a concave shape whereas those of baryons can be described reasonably well by a single exponential function. The comparison of the spectra from the two systems reveals a system size dependence of the slope parameters for the baryons.

$E_{kin} >= E_{thermal} + A * e_{collective}$. The slope of the curves in fig.2 determine $e_{collective}$ in a model independent way. The values are astonishingly high: 60% of the available energy is found in the collective expansion. This large fraction of kinetic energy helps to understand the large abundance of intermediate mass fragments that indicate a small entropy, although a quantitative description by statistical models has not been achieved so far [25].

For higher incident energies the long lever arm offered by the IMF emission is lost for central collisions. Beyond 1 AGeV the analysis is limited up to now to Hydrogen and Helium isotopes. Typical transverse mass spectra at midrapidity with a weighting factor of $1/m_t^2$ such that a thermal Boltzmann-like spectrum is represented by a straight line are shown in fig.3. Event samples of 120 mb ($b_{geo} = 2fm$) and 100 mb ($b_{geo} = 1.8fm$) on the basis of charged particle multiplicity were used for the Au+Au and Ni+Ni system, respectively. For this type of analysis the centrality selection is not as crucial any more, the results are already stable for the most central 400 mb ($b_{geo} = 3.6fm$). The proton and deuteron spectra can be described reasonably well by single exponential functions, while for the pion spectra the sum of two exponential functions is needed in order to describe the data. Comparing the slopes of the different ejectiles for the same reaction one observes an ordering according to the ejectile mass: π - specta are steeper than the proton spectra that themselves are exceeded by the deuteron spectra. It is also interesting to observe that at the same incident energy (1AGeV) the spectra change differently for different system sizes (Au+Au versus Ni+Ni). The variation of the slope parameter is

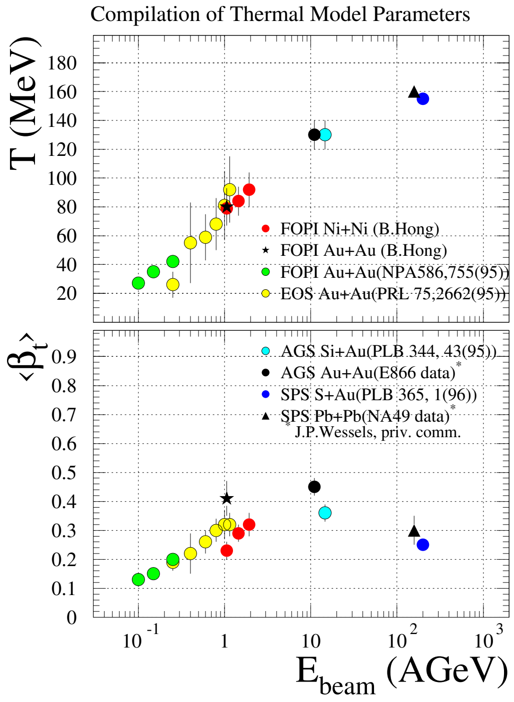

Figure 4. Excitation Function of Blast Model Parameters, Temperature T and average transverse expansion velocity β_t

larger for the heavier system.

The dependence of the slope parameter on the ejectile mass again is indicative for collective motion and motivates fitting the transverse mass distribution with a blast model hypothesis [26]. This approach was used lately by several authors. The summary of the available data in the energy range from 0.15 to 160 AGeV where the mass dependence of the slope parameters for the different particle species was used in order to extract the transverse flow component is shown in fig.4. Preliminary FOPI data [27] are shown in comparison to data from EOS [28] and AGS[29], SPS[30] including preliminary analysis of the heavy systems [31]. Plotted are the average transverse velocities and the accompanying temperatures that are obtained as a second parameter from the fits. It was checked that the results do not depend on the velocity profile, e.g. using a linear dependence of the flow velocity with the radius gave the same result as using a fixed expansion velocity as suggested in [26]. A clear trend is emerging from fig.4: the temperatures are logarithmically rising over the full incident energy range from 0.1 to 160 AGeV and do not show a system size dependence. The average transverse expansion velocities are rising from 0.1 to 2 AGeV and show a system size dependence at 1 AGeV (see fig.3). A similar feature is observed at the higher incident energies when comparing the different systems [31]. At 2 AGeV one observes collective expansion velocity values that are close to the ones obtained at an incident energy of 10.7 AGeV. The average transverse velocities seem to be limited to $<\beta_t>\leq 0.5$. Extrapolating from fig.4 the maximum should be located at an incident energy of around $E_{beam} = 5-10\,AGeV$.

It should be mentioned at this point that the analysis of the heavier fragments (Fig.2)

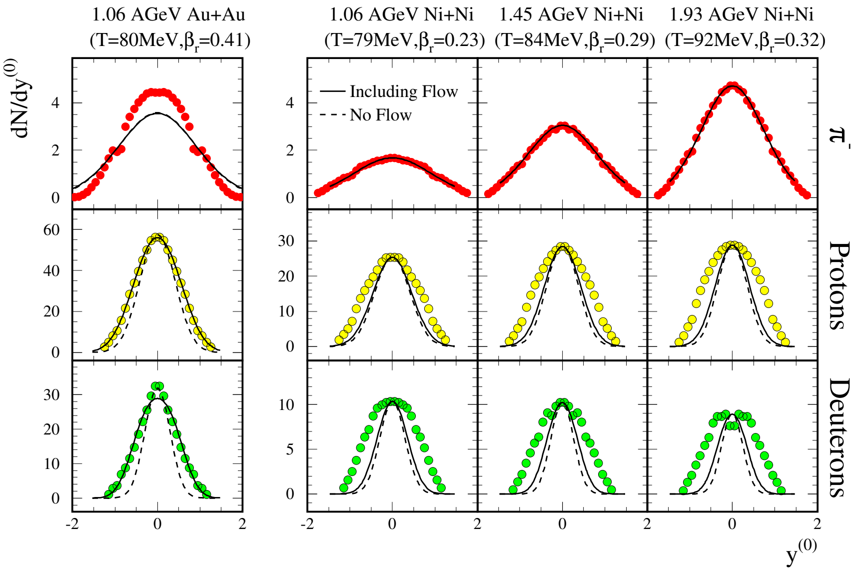

Figure 5. Rapidity Density Distributions

gives higher values for the average expansion velocities and accordingly lower temperatures. In trying to describe the distributions of heavier fragments with nuclear charges $2 \leq Z \leq 8$ with an isotropically expanding source [25], already at 400 AMeV an average expansion velocity of $<\beta>= 0.33$ is reached. This conclusion is in agreement with the light particle data [32] that are included in fig.4 and give a smaller value when analyzed for themselves. Their distributions are probably influenced by evaporation so that the mass dependence that gives rise to the collective flow estimate could be disturbed. Interestingly enough the spectra of the heaviest fragments show even a sensitivity to the flow velocity profiles at freeze-out. The exact shape of the excitation function on radial flow thus depends on the knowledge of the distributions of different particle species with a large mass lever asking for the future for an as complete measurement as possible with a special emphasis on the heavier fragments.

4. Stopping

Once a substantial part of the populated phase space is measured by the detector system, the question of nuclear stopping can be addressed. For the lower incident energies $E_{beam} \leq 0.4\, AGeV$ and the heavy system an isotropically radiating source can be identified [25]. For the energy range above 1 AGeV the situation is not so clear yet. Information can be extracted from the exponential fits to the transverse mass spectra like in Fig.3 that allow to estimate the total yield of the emitted particles by integrating the fit functions from 0 to infinity. The preliminary result of such an integration are shown in fig.5 for the system Au+Au at 1AGeV and for the system Ni+Ni at 1, 1.45 and 1.93 AGeV. The data are plotted versus the normalized center-of-mass rapidity $y^{(0)} = y/y_{projectile}$ and since for a symmetric system the forward and backward hemisphere in the CMS have to be the same are symmetrized around midrapidity. The data are compared to the predictions of an isotropic thermal model scenario with (solid lines) and without (dashed lines) radial

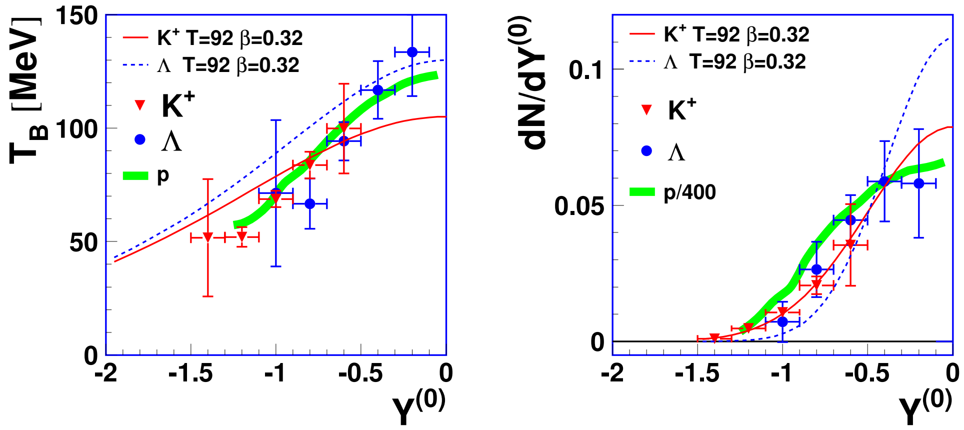

Figure 6. Slope Parameter and Rapidity Distributions of Strange Particles

flow. The parameters used for the different systems are the ones shown in fig.4 and are given in the figure.

Several interesting features can be noticed: The distributions of protons and deuterons for Au+Au at 1 AGeV are well described by an isotropically expanding source (with the parameter of the source determined by the transverse mass spectra at midrapidity). This Ansatz fails for the Ni+Ni system: a rapidity density distribution is observed that is wider than the one expected for an isotropically emitting source. While the data shown in fig.5 correspond to an integrated cross section of 100 mb this situation does not change even when selecting cross section as small as 30 mb. The enhanced longitudinal pattern is observed for the Ni system from 1 to 2 AGeV and indicates incomplete stopping. For the produced particles, e.g. pions, the deviations to the isotropic scenario are different: the data obtained for the different Ni measurements are compatible with the assumption of isotropic emission, while the pion distributions for the heavy system at 1 AGeV appear narrower than expected.

5. Production of Strange Particles

Since strangeness is conserved in strong interactions strange particles are expected to carry a more direct signal of the hot and dense state that is eventually reached in the course of the collision. Especially the K^+ with its long mean free path could serve as a messenger. Full phase space distribution are necessary in order to support this claim. Lately, the FOPI collaboration succeeded to identify strange particles within a 4π - detector at relative abundance of $1 \cdot 10^{-4}$ with respect to all particles [33]. Charged kaons are identified from a measurement of their specific energy loss in a central drift chamber, the curvature of the tracks and Time-of-flight of a scintillator barrel. Neutral strange particles are reconstructed from tracks that do not originate from the primary vertex and are identified from their invariant masses. The particle identification capability

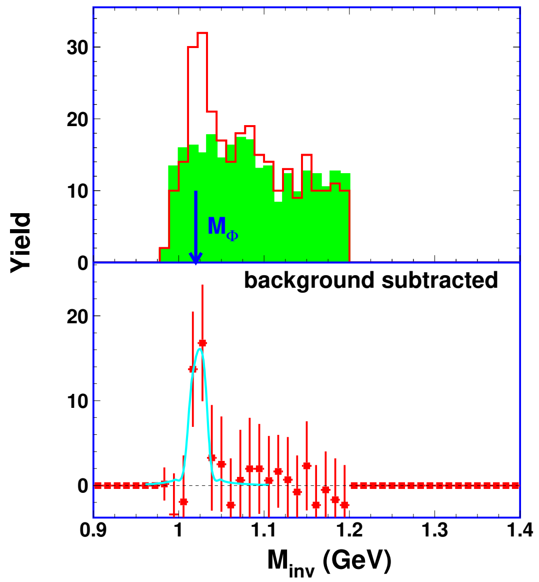

Figure 7. Invariant Mass Distribution of K^+-K^- pairs
The top panel shows the measured distribution as well as the one obtained from a mixed event analysis. The lower panel is obtained after subtraction of the uncorrelated background. The spectrum is artificially cut off at 1.2 GeV.

allows to discuss the distributions of strange particles (K^+ and Λ) directly in comparison to the baryon distributions. In order to bypass threshold and detection efficiency effects transverse mass spectra were fitted by exponential functions and slope parameter and yields are obtained. A comparison of the extracted parameters is shown in fig.6. Slope parameter (left panel) and integrated rapidity density distributions (right side) are shown for Protons, Kaons and Lambdas. Error bars reflect statistical errors only. A direct comparison to the protons show that the strange particle distributions are very similar a) in the slope parameter and b) with respect to the shape of the rapidity distributions. Both observations favour the claim for a kinetic equilibrium and/or substantial rescattering of the Kaons as well as of the Lambdas. On the other hand, within the framework of the expanding blast model scenario discussed so far, systematic differences are expected. The predictions for an isotropically emitting expanding source are given by the lines in fig.6, depicting the typical cosh(y) - behaviour for the slope parameters and almost gaussian shapes for the rapidity distributions. The K^+ - data are reasonably well described by the assumption of a radially expanding source while the Λ - data show systematic deviations that coincide with those observed for the protons. The slopes for rapidities $y^{(0)} < -0.5$ are smaller than expected whereas the rapidity distributions are more elongated (compare fig.5).

The phase space coverage of the FOPI - detector with simultaneous identification of all charged particles also allows to search for more exotic ones. In the context of strangeness production the most interesting one is the Φ - meson. This resonance can be reconstructed from its decay $\Phi \rightarrow K^+ + K^-$ with a branching ratio of 49.1%. Due to the narrow intrinsic width of $\Gamma = 4.4 MeV$ it can be recognized in the invariant mass distribution of $K^+ - K^-$ candidate pairs. The reconstructed invariant mass distribution is shown in fig.7 and shows a statistically significant enhancement at $M = 1.020\, GeV$ the mass of the free resonance. The combinatorial background was obtained from a mixed event analysis that employed

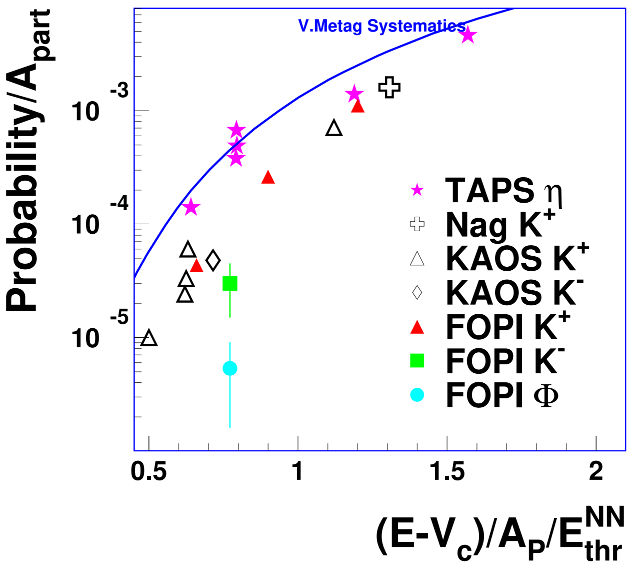

Figure 8. Comparison of Extrapolated Production Probabilities of Strange Mesons

the same cuts that were applied to the data. A total of 30 ± 8 Φ-mesons could be reconstructed in the reaction Ni+Ni at 1.93AGeV from an event sample of $7 \cdot 10^6$ events. This is certainly not sufficient to make any claims on their distributions but it is enough to get an estimate on the production yield and points to interesting options for the future.

In order to arrive at a meaningful comparison of the production rates of the different particles species one has to extrapolate to the full solid angle. For the lighter π and K-mesons an extrapolation prescription based on the blast model predictions can be justified by figs.5 and 6. For the Φ the same assumption of the emission from an isotropically emitting expanding source was used in order to determine the detection efficiency. The source parameter were determined from the baryon transverse mass spectra at midrapidity ($\beta = 0.32, T = 92MeV$). The overall detection efficiency was estimated from a MonteCarlo simulation of the complete detector response, tracking and identifying scheme starting with a thermal Φ-distributions with the parameters given above. Clearly much more statistics is needed to verify the assumptions and narrow down the systematic errors that are estimated to be smaller than a factor of 2, when neglecting the influence of the unknown angular distribution. Sensitivity to changes of the mean and the width of the peak requires a substantial increase in the statistics and thus dedicated running time.

Despite the difficulties discussed above it is instructive to compare the production yield for the different strange mesons. This is done in fig.8 where in addition to the directly observed Kaons and Antikaons and the estimate for the Φ of FOPI, recent data on K^+ and K^- from KaoS [34] and on η from TAPS [35] are included. The production probabilities per participant nucleon are plotted versus the incident energy above the Coulomb barrier normalized by the threshold energy that is necessary to produce a certain particle in a NN-collision. This representation was introduced by Metag [36] and yields a very consistent description for all the pion data from 0.02AMeV up to 2AGeV including the FOPI pions: it results in the solid line of fig.8.

Some preliminary conclusions can be drawn from inspection of fig.8:

- The production probabilities extrapolated from the FOPI data are consistent with those obtained at midrapidity with a dedicated spectrometer (KaoS [34]).
- The strangeness degree of freedom is not equilibrated, e.g. strange particles are not produced with a weight given by the mass relative to the corresponding threshold energy.
- The incident energy dependence seems to be stronger as compared to the pion systematics (given by the solid line).
- K^- and K^+ yield are comparable at the same available energy. This is surprising since the K^-- production is suppressed in pp collisions by an order of magnitude relative to K^+- production at the same available energy [34], e.g. when taking into account the different production thresholds in $pp \rightarrow nK^+\Lambda$ and $pp \rightarrow ppK^+K^-$.
- Φ - production occurs at a level of 10^{-2} to pions and 10% with respect to K^-. The later number is similar to observations made at AGS energies [37] and could be indicative for a coalescence like production mode.

The production probability systematics stresses the role of strange particles as a interesting probe for the properties of hot and dense hadronic matter. It should be noted that especially the observed production rate of K^- represents a puzzle since a) the elementary production rate is lower and b) the absorption is stronger as compared to K^+ [34]. Whether these losses can be balanced by additional production channels, e.g. $\Lambda\pi \rightarrow K^-N$, is questionable. In addition the phase space description fails to reproduce the various mass systems at the same incident energy. This deficiency is caused by a more than linear increase of the Kaon production yields with the number of participating nucleons [34,39], clearly indicating that central collisions are not just a superposition of independent NN - collisions.

A consistent model to describe all the available particle yields is not available yet. Most of the analyses have focused on the K^+ distributions so far. The comparison with transport models shows that $N\Delta$ and $\Delta\Delta$ collisions are necessary in order to account for the observed Kaon yield [40,41]. According to those models Kaons are predominantly produced in the early stages of the reaction at high temperature and densities. Since the elementary production cross sections are poorly known the uncertaintities in the quantitative conclusions are fairly large. The observed rates are, however, so large that a soft equation of state is needed in order to provide a sufficient number of collisions.

Whether one needs additional in-medium effect like the modification of the particle masses in order to explain the K^+ yields (like in [40]) is not clear at this moment. Modification of the (Anti)Kaon masses as they are expected from chiral perturbation theory could offer an explanation of the observed K^- yield. All the theoretical attempts dealing with in medium Kaon masses [8,9,40] predict a slightly rising Kaon and a more strongly dropping Antikaon mass when the baryon density is increased. K^- - mesons are therefore much more easily produced in dense matter.

Clearly those ideas need to be tested by independent observables. Within the framework of chiral perturbation theory dropping in-medium masses are caused by scalar and vector

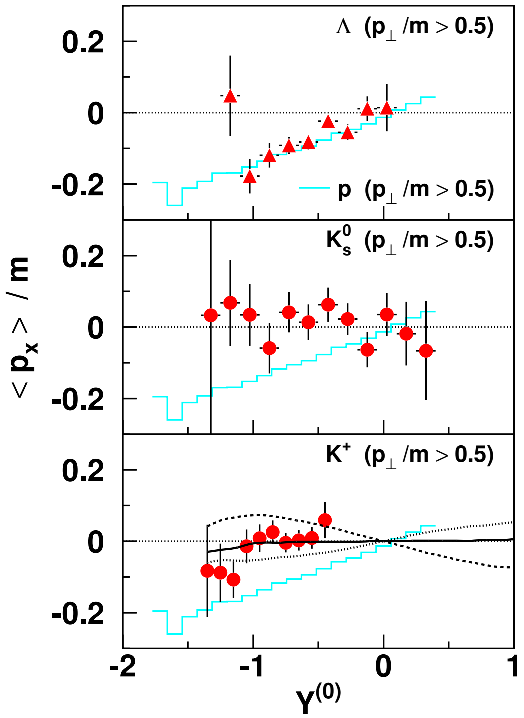

Figure 9. Sideward Flow of Strange Particles
Average transverse momenta per mass projected onto the reaction plane are shown as function of the normalized rapidity $y^{(0)}$ for Λ (top), $K°$(middle) and K^+ (bottom) in comparison to protons (histogram). The K^+ distributions are compared to the predictions from an RBUU calculation of Li and Ko [38] that make use of different in-medium potentials: the dashed dotted, dashed and solid lines represents the cases *no potential, vector potential only and scalar+vector potential*, respectively.

potentials that also influence the propagation of the particles through the matter [10]. It is therefore very important to try to measure the flow of the strange particles with respect to the baryon flow.

6. Strangeness Flow

First results on the directed sideward flow of strange particles have become available recently [33]. For the Ni+Ni reaction at 1.93 AGeV it is possible to determine the average in - plane momentum $< p_x >$ of Protons, Lambdas, K^+ and K^0 under the same kinematical cuts. The experimentally measured values are shown in fig.9 for a p_t/m - cut of 0.5 as function of the rapidity. The events used for this comparison were selected by means of charged particle multiplicity and represent the most central ones with an integrated cross section of 420 mb. The reaction plane resolution was determined to $\Delta\phi = 40°$. Note that the momentum cut enhances the $< p_x >$ value by more than a factor of 2 at target rapidity.

In all three panels protons are represented by the solid histograms. In the upper panel they are compared to Λ - particles. The distributions agree within the error bars and support the earlier observation that the phase space distributions of protons and Lambdas are very much alike. The middle and the lower panel of fig 9 shows the same comparison to the protons to K_s^0 and K^+, respectively. For both particle species no sideward flow signal is observed, e.g. the emission of those Kaons is independent of the orientation to the reaction plane. Since the production of Kaons and Lambdas at incident energies below 2 AGeV proceeds in an associate manner ($NN \rightarrow NK\Lambda$ or $N\Delta \rightarrow NK\Lambda$) the observed differences have to be attributed to the propagation process through the expanding nuclear medium. Λs seem to be attracted by the baryons whereas K^+ and K^0

are repelled.

The vanishing K^+ sideward flow was predicted by the RBUU transport model of Li and Ko under the assumption that both a scalar and a vector potential act on Kaons [10,38]. As can be seen from the bottom panel of Fig.9, where the model predictions folded with the experimental resolution are shown for various options of the Kaon potential, the data are incompatible with the assumption of free propagation of Kaons. According to the RBUU calculation the non-interacting Kaons should exhibit a small in - plane flow in the direction of the baryons. The origin of this sideward flow was traced to the production kinematics in NN and $N\Delta$ collisions [38]. The Kaons thus have to experience a force that repels them from the baryons. The comparison with the data shows that the vector potential is responsible for the repulsion, but it is too strong when it is not balanced at the same time by the scalar potential. The in-medium potentials also offer an explanation for the Λ-flow. In this case the potential is attractive and the Lambdas are pulled into the regions of high baryon density and pick up the relatively strong baryon flow [38]. Before taking the agreement as a proof for in-medium potentials it has to be mentioned there are indications that using a different transport code even without invoking in-medium potentials, the experimental findings can be described [42]. Clearly, a consistent comparison of the full event information is necessary before drawing final conclusions. An additional crucial test will be the extension of the current signals to Antikaons and the impact parameter dependence of the Kaon flow that will become available soon.

7. Summary and Conclusions

The amount of data available on heavy ion reaction around 1 AGeV has considerably improved and shows several remarkable features: a) The baryonic sideward flow is rising from 0.1 to 1 AGeV and seems to decrease or saturate above. b) The systems seem to explode with expansion velocities that are increasing in the incident energy range from 0.1 to 2 AGeV. c) Full stopping is only achieved for the heaviest system. d) Strangeness production in the near threshold region around 1-2 AGeV is not in chemical equilibrium, although the spectra of the strange particles are consistent with the assumption of a kinetic equilibrium. e) Differences between strange baryons and mesons are observed for the sideward flow. So far this full set of observations is not consistently accounted for by any dynamical theory. Since for some of the single observations like the K^- production rate fundamental changes of the properties of mesons in the nuclear medium seem to be necessary it remains a challenging task to compare all the available information to the predictions of theory consistently. This is especially important since at those energies one might have the unique opportunity to look at fairly low temperatures and high baryon densities at the consequences of fundamental symmetries of QCD, namely the partial restoration of chiral symmetry.

Acknowledgments

I would like to thank all members of the FOPI collaboration of SIS/GSI: B. Hong[4], J. Ritman[4], D. Best[4], A. Gobbi[4], K. D. Hildenbrand[4], Y. Leifels[4], C. Pinkenburg[4], W. Reisdorf[4], D. Schüll[4], U. Sodan[4], G. S. Wang[4], T. Wienold[4], J. P. Alard[3], V. Amouroux[3], N. Bastid[3], I. Belyaev[7], L. Berger[3], J. Biegansky[5], A. Buta[1], R. Čaplar[11], N. Cin-

dro[11], J. P. Coffin[9], P. Crochet[9], R. Dona[9], P. Dupieux[3], M. Dzelalija[11], M. Eskef[6], P. Fintz[9], Z. Fodor[2], A. Genoux-Lubain[3], G. Goebels[6], G. Guillaume[9], E. Häfele[6], S. Hölbling[11], F. Jundt[9], J. Kecskemeti[2], M. Kirejczyk[4,10], Y. Korchagin[7], R. Kotte[5], C. Kuhn[9], D. Lambrecht[3], A. Lebedev[7], A. Lebedev[8], I. Legrand[1], C. Maazouzi[9], V. Manko[8], J. Mösner[5], S. Mohren[6], W. Neubert[5], D. Pelte[6], M. Petrovici[1], F. Rami[9], V. Ramillien[3], C. Roy[9], Z. Seres[2], B. Sikora[10], V. Simion[1], K. Siwek-Wilczyńska[10], V. Smolyankin[7], L. Tizniti[9], M. Trzaska[6], M. A. Vasiliev[8], P. Wagner[9], D. Wohlfarth[5] and A. Zhilin[7]
[1] IPNE, Bucharest, [2] CRIP Budapest, [3] LPC Clermont-Ferrand, [4] GSI, Darmstadt, [5] FZ Rossendorf, Dresden, [6] Universität Heidelberg, [7] ITEP Moscow, [8] KI Moscow, [9] CRN and Université Strasbourg, [10] Warsaw University, [11] RBI Zagreb

REFERENCES

1. S.Klimt et al., Phys. Lett. **B 249** (1990) 386
2. G.E.Brown, M.Rho , PRL **66** (1991) 2720
3. T. Hatsuda, S.H.Lee, Phys.Rev. **C46** (1992) R34
4. G.Q.Li, C.M. Ko, Phys. Lett. **B338** (1994) 118
5. H. Yabu et al., Phys.Rev. **D50** (1994) 3549
6. J. Aichelin and C. M. Ko, PRL **55** (1985) 2661
7. D.B. Kaplan and A.E. Nelson, Phys.Lett. **B 175** (1986) 57
8. J. Schaffner et al., Phys. Lett **B 334** (1994) 268
9. M. Lutz et al., Nucl. Phys. **A574** (1994) 755
10. G.Q.Li et al., PRL **74** (1995) 235
11. G. Rai et al., IEEE Trans.Nucl.Sci. **37** (1990) 56
12. A. Gobbi et al.: Nucl. Instr. and Meth. **A324** (1993) 156,
    J. Ritman, Nucl. Phys. **B 44** (1995) 708
13. P.Senger et al., Nucl.Instr.Meth.Phys.Res. **A327** (1993) 393
14. R.Novotny et al., IEEE Trans.Nucl.Sci. **38** (1991) 379
15. R. Stock, Phys.Rep. **135** (1986) 259
16. H. Stöcker, W. Greiner, Phys.Rep. **137** (1986) 277
17. H.H. Gutbrod, A.M. Poskanzer, H.G. Ritter, Rep.Prog.Phys. **52** (1989) 1267
18. B. Blättel et al., Phys. Rev. **C43** (1991) 2728
19. J.Chance et al., submitted for publication, *http::/xxx.lanl.gov/nucl-ex/9607008*
20. A. Lang et al., Z.Phys. **A340** (1991) 287
21. P.Crochet, Phd thesis, CRN 96-09, Centre de Recherche Nucleaire, Strasbourg (1996)
22. K.G.R. Doss et al., PRL **57** (1986) 302
23. M.Partlan et al., PRL**75** (1995) 2100
24. S.C. Jeong et al., PRL **30** (1994) 3468
25. W.Reisdorf et al., submitted for publication
26. P.J.Siemens, J.O. Rasmussen, PRL **42** (1979) 880
27. B.Hong et al., to be published
28. M.A. Lisa et al., PRL **75** (1995) 2662
29. P.Braun-Munzinger et al., Phys.Lett. **B344** (1995) 43
30. P.Braun-Munzinger et al., Phys.Lett. **B365** (1996) 1
31. J.P. Wessels, private communication

32. G. Poggi et al., Nucl.Phys. **A586** (1995) 755
33. J. Ritman et al., Z. Phys. **A 352** (1995) 355
34. P.Senger et al., Proceedings of the Meson'96 Workshop, Cracow (1996)
35. R.Averbeck, private communication
36. V.Metag, Prog.Part.Nucl.Phys. 30 (1993) 75
37. B.Cole et al. (E859), Nucl. Phys. **A 590** (1995) 179,
    Y.Akiba et al., PRL **76** (1996) 2021
38. G.Q.Li et al., private communication
39. D. Miskowiec et al., PRL **72** (1994) 3650
40. X.S. Fan et al., Nucl.Phys. **A575** (1994) 766
41. C. Hartnack et al., Nucl.Phys. **A580** (1994) 643
42. J.Aichelin, private communication